Characterization of an Ultrahigh Peak Power $XeF(C \rightarrow A)$ Excimer Laser System

Thomas Hofmann, Tracy E. Sharp, *Student Member, IEEE,* C. Brent Dane, Peter J. Wisoff, *Member, IEEE,* William L. Wilson, Jr., *Senior Member, IEEE,* Frank K. Tittel, *Fellow, IEEE,* and Gabor Szabó

***Abstract*—The gain characteristics of an electron-beam pumped $XeF(C \rightarrow A)$ excimer amplifier operating in the blue-green spectral region were investigated for several laser pulse lengths. Saturation energy densities of 50 and 80 mJ/cm^2 were measured for injected laser pulse durations of 250 fs and ~100 ps, respectively. A gain bandwidth of 60 nm was observed with ~100 ps pulse injection. Using an optimized unstable resonator design, the laser amplifier has produced 275 mJ pulses with a pulse duration of 250 fs and a 2.5 times diffraction limited beam quality, making the $XeF(C \rightarrow A)$ amplifier the first compact laser system in the visible spectral region to reach peak powers at the terawatt level.**

Introduction

The development of high intensity amplifiers for subpicosecond laser pulses has become an area of considerable interest. To date, two different approaches to high power, ultrashort pulse amplification have been reported based on either excimer [1]-[7] or solid-state gain media [8]-[12]. Excimer based amplifier systems, operating in the ultraviolet spectral region, have been used successfully to generate output powers at the terawatt level. However, the small saturation energy density of ~2 mJ/cm^2 [13]-[15] for such systems requires large amplifier apertures in order to obtain high output powers. The small gain bandwidth of <5 nm for conventional rare gas-halide ultraviolet excimer systems restricts amplification of laser pulses to pulse durations longer than 80 fs. Solid-state laser systems, on the other hand, have large gain bandwidths in the infrared region of the spectrum and high saturation energies but exhibit optical nonlinearities, which limit the maximum allowable intensity in the amplifier. The introduction of chirped pulse amplification schemes [8] has circumvented this problem, although the damage threshold and availability of large recompression gratings still imposes design restrictions for solid-state based high power amplifiers.

The electron-beam pumped $XeF(C \rightarrow A)$ excimer amplifier, an attractive alternative to the above mentioned high power systems, has recently been demonstrated for ultrashort laser pulse amplification [16]. The blue-green $XeF(C \rightarrow A)$ transition is unique among conventional excimers because it is a bound-free transition with a highly repulsive lower state, which results in a broad linewidth and a small cross section for stimulated emission ($1 \cdot 10^{-17}$ cm^2) [17]. The $C \rightarrow A$ transition therefore exhibits a gain bandwidth (60 nm) and a saturation energy density (~50 mJ/cm^2) more than an order of magnitude larger than any other excimer currently used for short pulse amplification. Furthermore, the small optical nonlinearities of the gaseous gain medium permit the direct amplification of ultrashort pulses to high output powers.

The use of the $XeF(C \rightarrow A)$ excimer transition for an ultrashort pulse amplifier requires a comprehensive knowledge of the gain characteristics as a function of injected laser pulse duration. Extensive work on XeCl [13], [14] and KrF [15] excimer amplifier systems had shown a grouping of the gain characteristics into several temporal regimes. The shortest pulses that can be amplified are given by the Fourier transform of the gain bandwidth. For subpicosecond pulses, the molecular reorientation time of the gain, typically of several hundred femtosecond duration, prevents the full utilization of the stored energy for amplification [15]. This occurs because due to molecular rotation only a portion of the gain species can interact with the linearly polarized injection pulses. Repumping from vibrational and rotational levels and primary repumping from a discharge or an electron-beam excitation influence the amplification process on a picosecond and nanosecond time scale, respectively. All these effects depend strongly on the individual characteristics of the gain medium and knowledge of their behavior over a broad range of time durations is needed in order to accurately describe the excimer system.

Although the $XeF(C \rightarrow A)$ excimer gain has been extensively investigated for nanosecond laser pulses [18], [19], the gain characteristics in the picoseocond and femtosecond regime have only been measured recently [16]. In this paper the $XeF(C \rightarrow A)$ excimer gain for pulse durations between 250 fs and several hundred picosecond

Manuscript received May 15, 1991; revised September 4, 1991. The work of G. Szabó was supported by the OTKA Foundation of the Hungarian Academy of Sciences by Grant 3056. This work was supported by the Office of Naval Research, the Air Force Office of Scientific Research, and by the Robert Welch Foundation.

T. Hofmann, T. E. Sharp, P. J. Wisoff, W. L. Wilson, Jr., and F. K. Tittel are with the Department of Electrical and Computer Engineering, Rice University, Houston, TX 77251.

C. B. Dane is with Lawrence Livermore National Laboratory, Livermore, CA.

G. Szabó is with the Department of Optics and Quantum Electronics, JATE University, Szeged, Hungary.

IEEE Log Number 9106859.

0018-9197/92$03.00

pulse durations was measured, while in [16] we reported gain measurements with 800 fs pulses. Furthermore, the spectral gain characteristics for ~100 ps pulses and the first optimized energy extraction experiments using femtosecond pulses in a XeF($C \rightarrow A$) excimer amplifier are described.

Gain Measurement Setup

The experimental arrangement for the gain measurements is shown in Fig. 1. A probe beam of either 250 fs or ~100 ps duration was injected into an electron-beam pumped XeF($C \rightarrow A$) excimer amplifier. A detailed description of the XeF($C \rightarrow A$) excimer system is given in [18]. The dye laser injection beam was demagnified by an $M = 3$ telescope to a diameter of 1 mm in order to reach a sufficiently high energy density to investigate the XeF($C \rightarrow A$) gain saturation behavior.

The injection laser system for the femtosecond pulses consisted of a hybridly mode-locked dye laser, synchronously pumped by the third harmonic of a CW mode-locked Nd:YAG laser. The dye laser generated 800 fs pulses, tunable from 470 to 510 nm, that were subsequently compressed to 250 fs in a fiber-prism system. Tuning of the 250 fs dye laser system was limited to wavelengths greater than 488 nm due to the cutoff wavelength of the single-mode fiber employed. Amplification of these 250 fs, 50 pJ pulses in a two-stage dye amplifier, pumped by the third harmonic of a regenerative Nd:YAG amplifier, increased the pulse energy to 0.5 mJ [20].

For subnanosecond experiments, a simple dye laser oscillator was designed using a Littrow-grating, a transverse-flow dye cell, and a BK7 substrate as the output coupler. This laser and a subsequent dye amplifier stage were pumped by the 40 ps long, third harmonic output of the same regenerative amplifier used in the 250 fs dye amplifier configuration. The output of the dye laser system was ~1 mJ, and its tuning range from 450 to 530 nm, when using different dyes, covered the entire XeF($C \rightarrow A$) spectrum. Measurements of these pulses with a vacuum photodiode and a digital sampling scope gave an upper limit for the pulse duration of 250 ps. A lower limit of ~50 ps is estimated from the round trip time of the oscillator and the pump duration of 40 ps as determined with a streak camera. Since the XeF($C \rightarrow A$) gain characteristics are not expected to be very sensitive to the pulse duration within the described boundaries, the subnanosecond laser will be referred to as a ~100 ps source in the remaining text.

All optical elements for the gain measurements were made of fused silica to reduce induced absorption effects [16], except for the 9.5 mm thick excimer chamber windows, for which MgF_2 was chosen in order to avoid both absorption and self-focusing effects. The input and output energies of the amplifier were simultaneously monitored, using vacuum photodiodes which had been calibrated relative to one other. The accuracy of the gain measurements was limited by electrical noise from the electron-beam excitation and by the 1 Hz pulse repetition frequency of the amplifier, which limited extensive data averaging. All reported gain values have an estimated error margin of ±10%. The energy of the amplified pulses was additionally measured with a pyroelectric energy meter. For each pulse, the output beam profile at the gas cell window was imaged with a lens onto a CCD array and recorded.

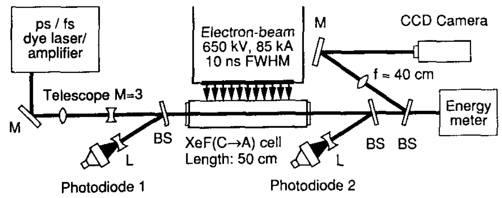

Fig. 1. Experimental apparatus for the measurement of single pass gain. The injection dye laser is either a 250 fs or a ~100 ps pulse duration system. *M*: aluminum mirror, *BS*: uncoated fused silica beam splitter, *L*: concave lens.

Revised Frantz-Nodvik Model

The Frantz–Nodvik model [21], which is widely used to describe the saturation behavior of short-pulse amplifiers, does not include the effect of gain saturation on the beam profile. When a beam in an amplifier approaches the saturation energy density, the center portion of that beam, due to its higher intensity, will experience a smaller gain than the outer region. As the beam travels through the amplifier, the beam profile will flatten out, resulting in an increased beam diameter. This effect is illustrated in Fig. 2 which shows the measured beam profiles of a 250 fs pulse both before and after being amplified in a saturating XeF($C \rightarrow A$) gain medium. The two profiles have been normalized for comparison. At the center of the input pulse, the peak fluence was about 150 mJ/cm^2. As is obvious from this, the amplified pulse profile is significantly broader and more flat-topped than the input pulse profile. Using full width at half maximum (FWHM) as a measure of the beam width in this situation would lead to an apparent doubling of the beam area and a subsequent overestimation of the saturation energy. For this reason, the saturation energy reported in [16] should be divided by a factor of 2. Spatial beam broadening due to gain saturation should be more pronounced for amplifier systems having a large gain-length product.

In order to achieve a more accurate saturation energy fit for the gain measurements and also to remove ambiguities in the definition of the beam area, a multidimensional variation of the Frantz–Nodvik model was used. The energy gain G can be calculated as [2]:

$$G = \frac{\int g(r) r E_{in}(r)\, dr}{\int r E_{in}(r)\, dr}$$

where $g(r)$ is the energy dependant gain factor, r is the radial coordinate, and $E_{in}(r)$ is the input energy density.

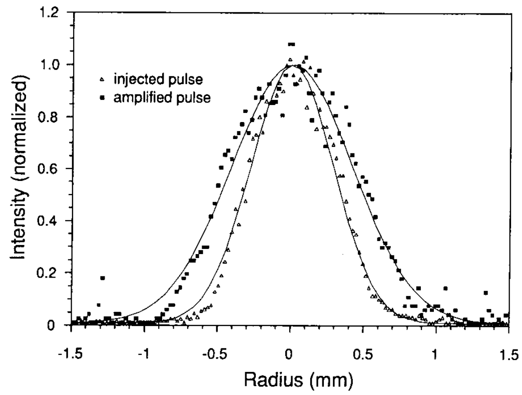

Fig. 2. Spatial profile of a 250 fs injection pulse and the resulting beam profile after amplification in a saturated gain medium. The shape of the injected pulse is fitted to a Gaussian curve and the solid curve for the amplified pulse is calculated using the revised Frantz–Nodvik model.

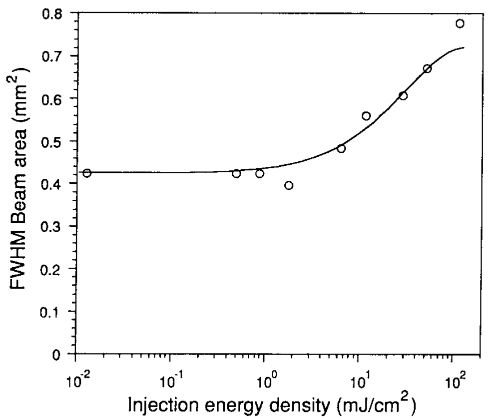

Fig. 3. Dependence of the beam area of a 250 fs pulse on the injected energy flux. The onset of gain saturation is clearly noticeable from the broadening of the amplified beam. The beam area is defined as the region where the intensity is larger than one half of the maximum intensity. The fitted curve was obtained by modeling the propagation of a Gaussian beam in a saturable amplifier having a saturation energy density of 50 mJ/cm^2.

When losses are neglected, $g(r)$ can be written as [14]:

$$g(r) = \frac{E_{sat}}{E_{in}(r)} \ln \left(1 + \exp(g_o L) \left[\exp\left(\frac{E_{in}(r)}{E_{sat}}\right) - 1\right]\right)$$

where $\exp(g_o L)$ is the small-signal gain and E_{sat} is the saturation energy density. The neglection of diffraction effects by this model is justified, because at a beam diameter of 1 mm and a gain length of 50 cm the propagation of the beam is entirely in the near field.

To check the validity of this approach, the change in beam diameter as a function of injected energy density was calculated and compared with experimental data. As shown in Fig. 3 the calculations provided a good fit to the measured values. The saturation energy density was the only free parameter used in the fit and can therefore be evaluated by monitoring the beam profile of the amplified pulse. The main purpose of developing this model, however, was to give a more reliable Frantz–Nodvik fit for the dependence of output energy on input energy.

Gain Measurements

In order to study the spectral characteristics of the XeF($C \rightarrow A$) excimer transition using short laser pulse injection, the gain was measured in the region from 450 to 530 nm with ~100 ps long laser pulses. As shown in Fig. 4, the single pass gain for ~100 ps, 1 mJ/cm^2 laser pulses is characterized by a smooth spectral profile with a FWHM of 60 nm. This is similar to the bandwidth obtained with nanosecond pulse injection [22]. The significance of a smooth spectral gain dependence becomes apparent when one looks at the spectrum of the free running XeF($C \rightarrow A$) excimer laser as also displayed in Fig. 4 [22]. The broadband laser spectrum exhibits several narrow absorption bands, primarily due to excited argon, krypton, and xenon atoms created during the electron-beam excitation [19]. These absorption bands limit the gain bandwidth, and can therefore restrict amplification of ultrashort pulses. If it is possible, however, to saturate these absorbers, the full bandwidth of the XeF($C \rightarrow A$) transition would be available for amplification. Most of the absorbing species have a larger absorption cross section than the XeF($C \rightarrow A$) transition and therefore saturate at lower fluxes than the gain does. This effect was demonstrated with nanosecond gain measurements [19] at a narrowband absorber wavelength, where the gain actually increased with higher injected intensities. The smooth gain profile in Fig. 4 therefore clearly indicates saturation of the atomic narrowband absorbers, which makes the entire XeF($C \rightarrow A$) bandwidth accessible for tunable narrowband or ultrafast, large bandwidth amplification at high energy densities.

Saturation of excited rare gas absorbers at high energy densities was also predicted by a coherent interaction model for the XeF($C \rightarrow A$) excimer amplifier [23]. According to this model, it appears possible to bleach out even broad-band absorbers, primarily photodissociating excited xenon atoms, due to their twice as large optical cross section compared to the XeF($C \rightarrow A$) transition.

The dependence of gain on energy density was measured for both 250 fs and ~100 ps pulses and is shown in Fig. 5. The measurements were performed in a single pass through the 50 cm long active gain medium. The probe wavelength in each case was 490 nm, representing one of the peaks in the free running XeF($C \rightarrow A$) laser spectrum shown in Fig. 4. The single pass gain for the ~100 ps pulses was measured to be 5.7 which corresponds to a gain coefficient of 0.034 ± 0.003 cm^{-1}. The saturation energy density was calculated to be 80 mJ/cm^2 using the modified Frantz–Nodvik model described previously. The same model applied to the 800 fs data [16] yielded an identical small-signal gain and saturation energy density. This implies that no significant gain repumping occurred on a 1–100 ps time scale.

Measurements with the 250 fs laser probe pulses yielded

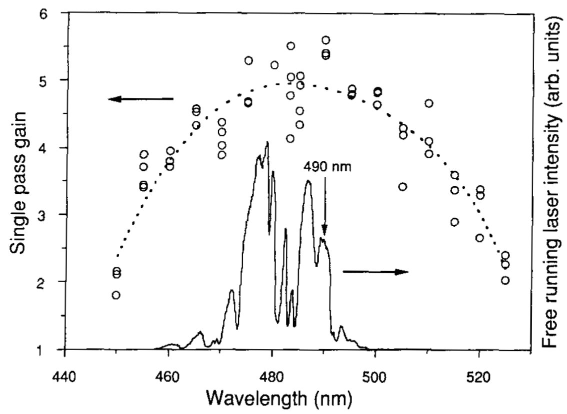

Fig. 4. Spectral dependence of the XeF($C \rightarrow A$) excimer single pass gain for injection pulses of ~ 100 ps duration. The gain length was 50 cm and the injected energy density was 1 mJ/cm^2. The spectrum of the free-running nanosecond laser (amplifier ASE spectrum) is shown for comparison. The gain spectrum shows a smooth profile with no apparent influence of the narrowband transient atomic absorptions observed in the laser spectrum.

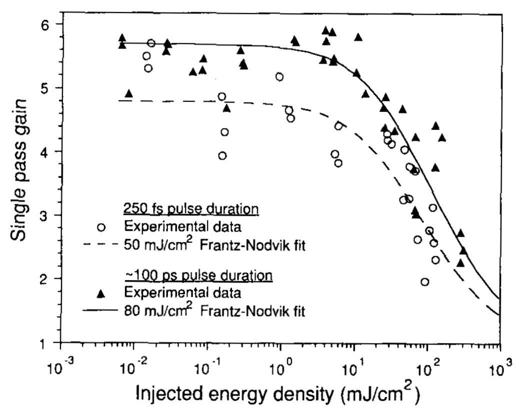

Fig. 5. The dependance of single pass gain of a 50 cm long XeF($C \rightarrow A$) excimer amplifier on the injected energy density for 250 fs and ~ 100 ps pulse durations at a wavelength of 490.5 nm. The Frantz-Nodvik curves were fitted taking into account beam-broadening effects.

a saturation energy density of 50 mJ/cm^2, which is in excellent agreement with predictions of a theoretical model [23] and also agrees well with the saturation energy density of 40 mJ/cm^2, calculated from the cross section for stimulated emission [17]. The small-signal gain was slightly smaller for the shorter pulse duration, although the difference of the gain values is within the measurement accuracy.

A decrease of the saturation energy density for 250 fs pulses was expected, since the rotational reorientation time of the XeF(C) excimer, estimated to be approximately 0.8 ps [16], allows saturation of only a portion of the polarization distribution of the gain medium. On a longer time scale, the orientational distribution relaxes, leading to a partial recovery of the gain for the probed polarization. This also explains the discrepancy between the saturation energy densities measured for 100 ps pulse durations and estimated from the cross-section for stimulated emission. The Frantz–Nodvik theory does not consider gain repumping effects, resulting in a larger fitted saturation energy density. Molecular reorientation becomes important only when the gain is partially saturated and has no effect on the small-signal gain.

In addition to gain measurements, further investigations were performed on the effect of beam confinement in the XeF($C \rightarrow A$) amplifier medium at high energy density levels. This effect was first observed for 800 fs pulses [16]. At high energy densities the beam profile of amplified 250 fs pulses developed a narrow central spike, only one tenth the width of the initial beam diameter and containing less than 6% of the total energy. For pulses of 490.5 nm wavelength the onset of beam confinement occurred at about 120 mJ/cm^2, corresponding to an intensity of 600 GW/cm^2. The laser optics used in the system were tested separately for this effect and did not exhibit any beam narrowing for energy densities up to 4 J/cm^2 [16], confirming that the spatial narrowing takes place in the excimer gas.

The measured intensity threshold for beam confinement for 250 fs pulses and the resulting beam profiles are very similar to the results obtained with 800 fs pulses. When using the ~ 100 ps pulse laser as an injection source, no beam confinement was observed for energy densities as high as 500 mJ/cm^2 and intensities of up to 5 GW/cm^2 at a wavelength of 490 nm, indicating an intensity rather than an energy dependence of the beam narrowing effect.

Self-focusing is a well-understood phenomenon in solid-state laser amplifiers and a measure of the self-focusing that occurs in a medium of length L is given by the B-integral [24]:

$$B = \frac{2\pi}{\lambda} \int_0^L n_{2I} I \, dL$$

where n_{2I} is the intensity dependent nonlinear index of refraction of the gain medium. This integral gives the number of phase shifts, accumulated in the amplifier due to the nonlinear refractive index. An empirical value for the B-integral of smaller than 3 is regarded necessary to avoid self-focusing.

In the XeF($C \rightarrow A$) gas mixture, the primary contributions to the nonlinear refractive index can be assigned to argon and krypton, which were contained in the amplifier cell at partial pressures of 5.5 and 1 bar, respectively. Using a nonlinear refractive index for argon of $9.1 \cdot 10^{-20}$ cm^2/W · atm and for krypton of $2.5 \cdot 10^{-19}$ cm^2/W · atm [25] together with an intensity in the amplifier of 600 GW/cm^2, the value for the B-integral is calculated to be ~3. Therefore, the observed beam confinement effect in the XeF($C \rightarrow A$) amplifier is most likely a result of the optical nonlinearity of the gas mixture. Self-focusing strongly depends on the intensity, and therefore on the saturation energy density, of the amplifier. For this reason, in other gas laser amplifiers with smaller saturation fluences, no self-focusing has been observed.

Due to the high energy threshold for self-focusing of approximately three times the saturation energy density, the applicability of the XeF($C \rightarrow A$) excimer transition for 250 fs pulse amplification is not expected to be compromised, if the peak intensity can be controlled by a proper amplifier design. Self-focusing, rather than the saturation energy density, however, is expected to become the limiting factor for high power amplification with the XeF($C \rightarrow A$) amplifier for pulse durations shorter than 90 fs.

Amplifier Design

The primary goal in the design of a femtosecond amplifier based on the XeF($C \rightarrow A$) excimer transition was to achieve high energy extraction efficiency from the gain medium. Also of consideration, however, was that this extraction should be achieved with good beam quality to provide optimal focusability for high intensity material interaction studies. The XeF($C \rightarrow A$) excimer system used in these experiments was capable of producing nanosecond duration output pulses of 1 J energy at a pulse repetition frequency of 1 Hz when it was operated as an injection-controlled laser [26]. The saturation energy density of 50 mJ/cm^2 reported here and an amplifier aperture of ~ 12 cm^2 was expected to yield a comparable output energy even for subpicosecond injection laser pulses. Since the dye laser injection system generated output pulses of 250 fs duration with an energy of 0.5 mJ, a 1000 to 2000 times amplification was required in order to access the projected energy storage capability of the XeF($C \rightarrow A$) amplifier. For a small-signal, single pass gain of 5, this translated to a 4 to 5 pass amplifier configuration.

A positive-branch confocal unstable resonator, similar to that successfully used for nanosecond injection control of the XeF($C \rightarrow A$) excimer laser [22], was chosen for the short pulse amplification experiments. By injecting the seed pulse through a small hole centered in the coating of the concave reflective optics, no active optical switching such as that used in more complicated regenerative amplifier configurations was required. By using injection apertures a few mm in diameter, the available dye laser pulse energy resulted in an injection fluence near the measured saturation energy density. The spatial beam expansion, as determined by the resonator magnification was closely matched to the XeF($C \rightarrow A$) gain coefficient resulting in an almost constant fluence of the beam throughout the amplification process. The constant, high fluence provides for both optimum energy extraction efficiency and for saturation of narrowband absorption along the entire amplification path.

Since the afterglow gain in the XeF($C \rightarrow A$) e-beam pumped excimer medium only lasted for ~ 10 ns, it was also desirable to minimize the optical transit time outside of the gain region. In this respect, another advantage of the unstable resonator was the ability to bring the mirrors very close to the 50 cm active medium. One possible disadvantage of this approach is that it did not readily allow amplified stimulated emission (ASE)-reducing elements to be placed between amplifier passes, an only minor concern for a low gain system such as the XeF($C \rightarrow A$) excimer amplifier.

Initial experiments using the low magnification unstable resonator with a 1.5 mm injection aperture described in [22] resulted in the formation of up to five output pulses for a single injection pulse. Not only are these multiple pulses undesirable for many potential applications, but they also reduce the maximum available output power in any one pulse. To obtain a detailed understanding of the source of these pulses, a three-dimensional optical propagation analysis was undertaken using a physical optics computer code. The results of these calculations confirmed that diffraction effects were the primary sources of the multiple output pulses. To achieve acceptable input coupling to the unstable resonator, the injection hole in the concave reflector must be overfilled. Diffraction effects on the hard edges of this hole, however, were discovered to have a significant impact on the multipass propagation through the amplifier. In general, resonators with larger magnification and hence fewer round-trips in the resonator are less sensitive to the development of multiple pulses. However, the magnification must be adjusted to the size and duration of the small-signal gain and is usually not a free parameter in the resonator design.

A good qualitative understanding of the generation of multiple output pulses can first be gained from a simple ray tracing analysis. In an ideal confocal resonator with a nondiverging input beam, every two adjacent beams traveling in the same direction are spatially separated [Fig. 6(a)]. Neglecting diffraction, a properly chosen output coupler diameter insures that only the final-pass annular beam leaves the cavity. When the input beam is divergent, however, adjacent beam passes overlap [Fig. 6(b)] and can no longer be separated by the output coupler, resulting in multiple output pulses, temporally separated by the resonator round-trip time. The ray tracing analysis suggests that a decrease in the cavity length from the confocal mirror spacing results in an increased divergence of the beams inside the resonator and thus provides better spatial separation between adjacent beam passes [Fig. 6(c)]. Since possible remaining overlapping beam regions resulting from a slight divergence in the input or diffraction from the injection aperture lie at the innermost part of the output beam, this region could be masked with an oversized output coupler with only a small reduction in overall output aperture.

Fig. 7(a)–(c) illustrates the effect of an increasing injection aperture diameter as calculated in the detailed diffraction propagation analysis. For each injection hole size, the cavity magnification was set so that a beam 4 cm in diameter emerged from the resonator after 5 single passes. Injection holes of 1.5, 2, and 2.5 mm in diameter therefore resulted in magnifications of 5.2, 4.5, and 4.0, respectively. The diameter of the output coupler was adjusted to the size predicted to result in single pulse output from a simple ray tracing analysis. As demonstrated, the

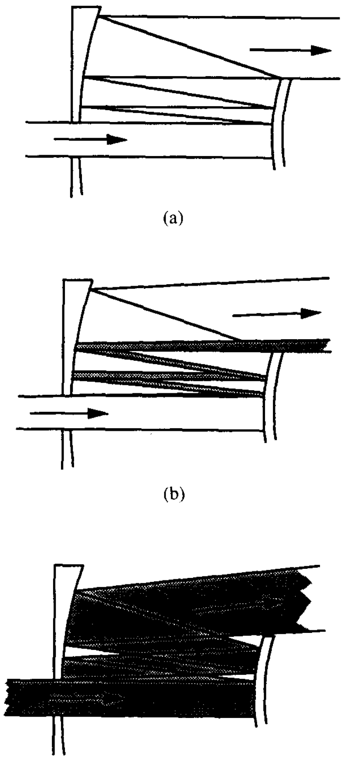

Fig. 6. The ray tracing beam paths of an injected pulse in an unstable resonator. (a) A nondiverging beam in a confocal unstable resonator. Beams traveling in the same direction do not overlap. (b) Same as in (a) but for a diverging input beam. The beam paths overlap as displayed in the hatched region and cannot be separated by the output coupler, resulting in multiple output pulses. (c) Same as in (b) but for a cavity length shorter than confocal separation. The imposed divergence in the resonator separates the beam paths, leaving only one output pulse. The hatched region represents the beam path.

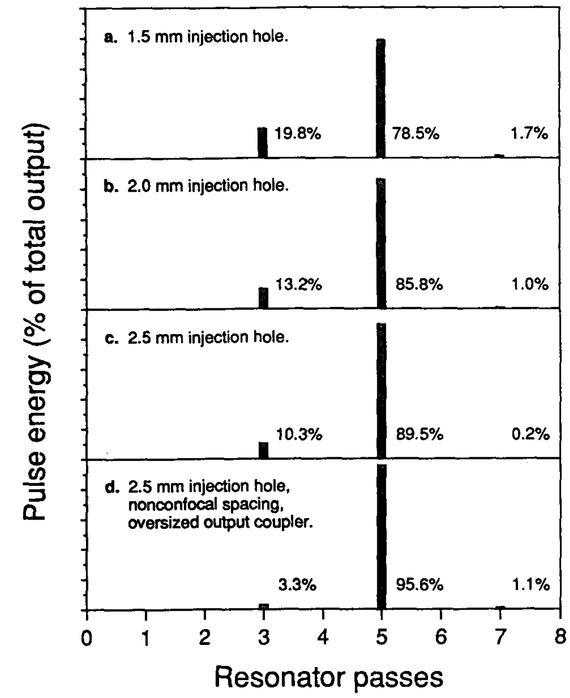

Fig. 7. A summary of the effect of resonator injection hole diameter as computed by the diffraction propagation analysis. Each bar represents the integrated relative energy of the 3-D beam intensity profile. For each aperture size, the resonator magnification and output coupler diameter were set such that ray tracing predicts a single output beam 4 cm in diameter that emerges after 5 resonator passes. (a) 1.5 mm injection hole, 5.2 cavity magnification, 7.7 mm output coupler, and a 67 cm mirror spacing. (b) 2.0 mm injection hole, 4.5 cavity magnification, a 8.9 mm output coupler, and a 67 cm mirror spacing. (c) 2.5 mm injection hole, 4.0 cavity magnification, a 10 mm output coupler, and a 67 cm mirror spacing. (d) The single pulse performance of the resonator described in (c) can be improved further by reducing the mirror separation from the confocal spacing of 67 cm to 57 cm and by increasing the output coupler diameter to 12.5 cm.

energy in the transmitted pulses leading and following the main pulse was calculated to be significantly reduced by increasing the injection aperture from 1.5 to 2.5 mm. The effect is partially masked by the decreasing cavity magnification with increasing injection hole diameter. Even so, this leads to the conclusion that the ideal injection hole diameter should be as large as possible without reducing the injection fluence to a level that the extraction efficiency is significantly compromised.

As suggested from ray tracing, improved performance should also result from a shorter than confocal mirror spacing. When the resonator mirror spacing was shortened from the confocal spacing of 67 to 57 cm and the output coupler was increased in diameter from 10 to 12.5 cm, the secondary pulses were predicted to be attenuated further to a level of only a few percent of the main pulse as illustrated in Fig. 7(d). Of significant consequence also is that the shorter unstable resonator was calculated to be much less sensitive to the dye laser injection beam divergence and hence to the precise adjustment of the collimating input telescope. Fig. 8 presents the diffraction calculation analysis of the relative size of the prepulse with respect to the input divergence. The divergence scale represents divergence due to spherical curvature on the in-

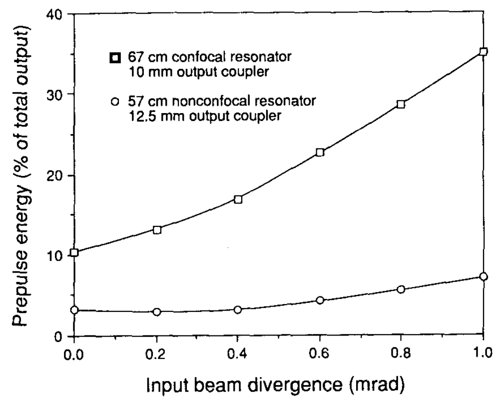

Fig. 8. The calculated sensitivity of the resonator of Fig. 7(c) and that of Fig. 7(d) to the divergence of the injection beam. The divergence scale represents divergence due to spherical curvature on the injection beam, therefore a value of zero represents a flat phase front at the injection aperture.

jection beam. Therefore, a value of zero represents a flat phase front at the injection aperture.

In addition, the amplification process has a significant influence on the absolute size of emerging pre- and post-pulses. Prepulses will experience at least two passes less through the gain medium and will therefore be attenuated by a factor of approximately 30 relative to the main pulse. However, an increase in the post-pulse energy due to additional amplifier passes is not likely both because of the limited gain lifetime and because of considerable gain saturation by the main pulse.

For these experiments, a five pass resonator was constructed with a magnification $M = 4$ and a cavity length 15% shorter than confocal (from 67 to 57 cm). A slightly oversized output coupler 12.5 mm in diameter was specified, which reduced the effective output area (12 cm^2) by only ~3%. Unfortunately, due to manufacturing tolerances, an 11 mm diameter coated spot was obtained. However, this reduction in diameter was calculated to have only a small effect on the observed resonator performance. The resonator coatings were highly reflecting from 470–530 nm and had a high transmission at the competing 249 nm KrF($B \rightarrow X$) and 353 nm XeF($B \rightarrow X$) excimer wavelengths.

Energy Extraction

For energy extraction measurements, an optimized unstable resonator as described above was used. The optical damage threshold of the resonator mirrors for 250 fs pulses was measured to be ~1 J/cm^2, which is an order of magnitude larger than the highest flux in the amplifier cavity. The neutral density filters used to attenuate the dye injection beam were tested prior to the gain measurements and did not exhibit saturation at the highest injection intensity. The pulse energy injected into the XeF($C \rightarrow A$) amplifier for extraction studies was measured on each shot with a calibrated photodiode and a transient digitizer. The total output energy was measured with a pyroelectric energy meter.

The energy extraction from the XeF($C \rightarrow A$) excimer amplifier was investigated with 250 fs long laser injection pulses at a wavelength of 490.5 nm. Only one output pulse was observed with a photodiode with 300 ps resolution. Multiple pulses, separated by the cavity round-trip time of 4 ns, were not detected with the available signal to noise ratio of 20. The dependence of the output energy of the XeF($C \rightarrow A$) amplifier on the injected energy is shown in Fig. 9. A maximum output energy of 275 mJ was obtained with an injection energy of 0.5 mJ. The solid line in Fig. 9 depicts the amplifier output energy calculated by a numerical model, based on gain lifetime [16] and gain saturation measurements. Fig. 10 shows the same experimental and calculated data as in Fig. 9, but plotted in terms of the amplifier gain as a function of the injected laser pulse energy. The measured saturation behavior of the amplifier is in good agreement with predictions derived from single pass gain measurements. It is apparent

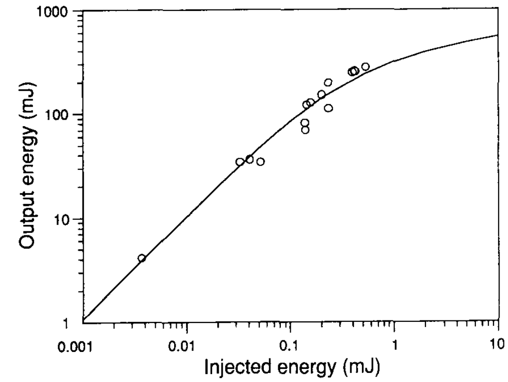

Fig. 9. The dependence of the output energy of the XeF($C \rightarrow A$) excimer amplifier on the injected energy for 250 fs pulses at a wavelength of 490.5 nm. The solid line is calculated from gain saturation measurements.

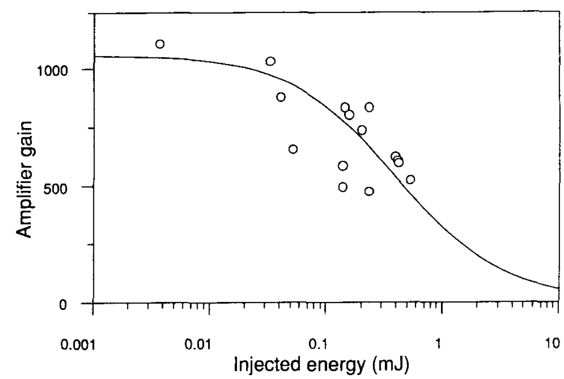

Fig. 10. Same data as Fig. 9, but plotted as a function of the XeF($C \rightarrow A$) amplifier gain versus the injected laser energy. The solid line is calculated from gain saturation measurements.

from Fig. 10 that the amplifier is driven into moderate saturation at maximum output, resulting in good energy extraction efficiency. Deep saturation was avoided in order to prevent temporal pulse broadening.

The highest energy achieved with amplified 250 fs pulses was about one quarter of the maximum energy of 1 J as observed for nanosecond injection [26]. This represents a good energy extraction efficiency for a femtosecond amplifier and underlines the importance of a large saturation energy density. The reduced energy with short-pulse injection, as compared to the nanosecond laser, results for a number of reasons. The effective life time of the XeF(C) excimer in a high pressure buffer gas is of the same order as the pump duration (10 ns FWHM) and therefore contributes to losses if the gain is not rapidly depleted by a continuous light flux. Furthermore, the molecular reorientation time of the XeF(C) excimer prevents the full usage of the stored energy with 250 fs long linearly polarized laser pulse injection. And finally, the nonuniform near field profile of the amplifier output, as described later, restricts the applicable average energy density to a relatively modest level, in order to avoid deep gain saturation at peak intensity regions.

The pulse durations of both the injected and the amplified pulses were measured with a phase-sensitive single-shot autocorrelator [27]. The observed pulse durations exhibited shot-to-shot fluctuations caused by the sensitivity of the fiber pulse compressor to fluctuations in the energy output of the oscillator for the injection system [20]. However, since minimum pulse durations of 250 fs were observed for both the injected and the amplified pulses, no temporal broadening of the pulses due to the amplification process was apparent. Fig. 11 shows an autocorrelation trace of an amplified pulse of 200 mJ energy. The trace can be fitted by a 250 fs pulse with a double sided exponential pulse profile, which confirms generation of output powers at the terawatt level by the XeF($C \rightarrow A$) excimer amplifier.

For an estimation of the ASE level of the XeF($C \rightarrow A$) amplifier, the output was measured with the injection beam blocked. An isolated measurement of only the final amplifier is justified, since the injection dye system has been shown to produce less than 0.1% of ASE output [20]. The energy meter was placed at a distance of 4 m from the amplifier and had an effective detector area closely matched to the size of the amplified beam.

An ASE pulse of <1 mJ energy and of 20 ns duration was observed. This corresponds to an ASE level of $<0.4\%$ and an intensity contrast ratio of $2 \cdot 10^7$ between the amplified output and the ASE. The measured ASE energy should be regarded as an upper limit, since gain saturation due to an injected laser beam is likely to reduce ASE. It is expected that spatial and spectral filtering of the amplified beam or the use of a saturable absorber would result in a significant increase of the contrast ratio.

The spatial beam profile after amplification was recorded with a CCD camera in an arrangement similar to one used for the gain measurements. The observed beam profile exhibited no indication of beam confinement. This is in agreement with the relatively small peak energy density of ~ 50 mJ/cm^2 in the amplified beam as compared to the previously observed threshold for filamentation of ~ 120 mJ/cm^2. The beam profile showed an intensity twice as high as the average at locations adjacent to the electron-beam pump side. This is due to the single-sided, transverse electron-beam excitation of the pump configuration employed, which creates a gain gradient perpendicular to the optical axis and results in a nonuniform amplified beam [18].

The divergence of the amplifier output was measured both with and without the electron-beam excitation. The output beams were focused by a 4 m lens and the far-field spot size was observed by placing a CCD camera in the focal plane of the lens [28]. The beam intensity was attenuated by using the front surface reflections of three wedged beamsplitters and by additional neutral density filters.

Fig. 12 depicts the experimentally measured profiles of the injection and amplified pulses indicating no measurable change in divergence after amplification, even given the $\sim 2:1$ intensity gradient across the beam described previously. This is consistent with the numerical simulation of the far-field patterns. Also presented are the theoretically predicted diffraction-limited far-field profiles of a 4 cm tophat beam with an 11 mm obscuration (our ideal experimental profile) and of a Gaussian beam with a $1/e^2$ diameter of 4 cm. Each profile is normalized to the same peak height. When the 3-D profiles are integrated and normalized to the same energy, it is found that the experimentally measured peak intensity is $\sim 40\%$ of that predicted for the diffraction limited annulus and $\sim 18\%$ of the Gaussian peak intensity. This implies that the amplified high power pulses in this study have the same focusability as a Gaussian beam whose diameter is 2.4 times smaller than that of our annular beam. It is important to note that since the injected and amplified beam divergences were equivalent, the measured beam quality is limited by that of the injection laser and the accuracy of the resonator optics. It therefore does not represent a fundamental limitation by optical aberrations that might be

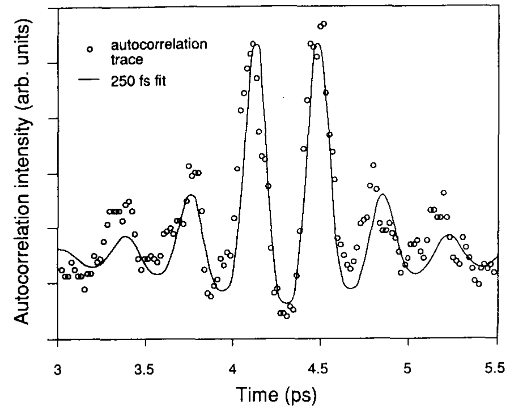

Fig. 11. Phase-sensitive single-shot autocorrelation trace of an amplified pulse. The output pulse energy is 200 mJ. The fitted curve represents a 250 fs pulse of double-sided exponential shape.

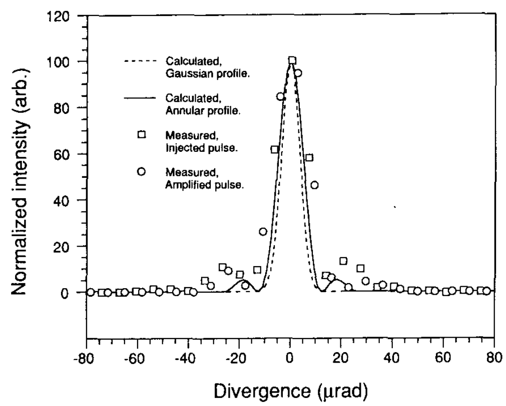

Fig. 12. Measured far field profiles of the injected (□) and the amplified (○) XeF($C \rightarrow A$) laser output as experimentally recorded at the focus of a 4m plano-convex lens. The solid line represents the calculated divergence of a Gaussian profile with a $1/e^2$ diameter of 4 cm and the dashed line is the calculated divergence of a 4 cm annular tophat beam with an 11 mm central obscuration. The peak height of each profile is normalized.

present in the gain medium and could be improved. Assuming a 2.4 times diffraction limited beam and an output power of 1 TW, the use of an $f/1$ parabolic reflector could result in a laser intensity at the focal point in excess of 10^{18} W/cm^2.

Conclusion

The spectral and energy dependance of the gain of the XeF($C \rightarrow A$) excimer transition has been characterized over a wide range of pulse durations. The spectral gain profile was measured for ~100 ps injection pulses and was found to have the same FWHM bandwidth of 60 nm as observed in the nanosecond pulse regime. Narrowband absorbers could be completely saturated, resulting in a smooth gain profile necessary for ultrashort pulse amplification and wide-band tuning.

The gain characteristics of the XeF($C \rightarrow A$) excimer transition were investigated for pulse durations of 250 fs and ~100 ps and compared to previous 800 fs and nanosecond measurements. The gain coefficient of 0.034 $\pm$ 0.003 cm^{-1} and the saturation energy density of ~80 mJ/cm^2 were found to be virtually independent of the pulse duration for pulses as short as 800 fs. For 250 fs pulses the gain coefficient decreased by 10% and the saturation energy density decreased to ~50 mJ/cm^2.

The XeF($C \rightarrow A$) saturation energy density is larger by a factor of 20 to 30 compared to that measured for conventional $B \rightarrow X$ excimers [13], [15]. This allows for an improved energy extraction for a given amplifier area and a higher overall amplifier efficiency. In particular, the high saturation energy density for 250 fs injection pulses permits efficient direct amplification of such pulses to the terawatt level. Furthermore, the small gain coefficient of the XeF($C \rightarrow A$) excimer transition facilitates suppression of ASE in such an amplifier.

Intensity dependant beam confinement in the XeF($C \rightarrow A$) excimer gas was observed for 250 fs pulses above an energy density threshold of ~120 mJ/cm^2. No confinement occurred with ~100 ps pulses at even higher energy densities.

An unstable resonator was designed for optimized femtosecond pulse energy extraction from a XeF($C \rightarrow A$) excimer amplifier. This resonator was especially adapted to the low gain medium and to the generation of a single pulse output. Amplification of 250 fs pulses resulted in an output energy of 275 mJ with an ASE background of less than 0.4%. The beam quality of the amplified pulses is close to the beam-shape-determined diffraction limit, yielding good focusability and the potential for the generation of ultrahigh intensities.

The amplification of 250 fs pulses with ~2 nm bandwidth made use of only a fraction of the XeF($C \rightarrow A$) gain bandwidth of 60 nm. It is expected that pulses of much shorter duration, such as the blue-green 10 fs pulses demonstrated by Schoenlein *et al.* [29] or frequency-doubled mode-locked Ti:sapphire pulses could be amplified in this excimer system, possibly further increasing the peak output power. In fact, modeling of the XeF($C \rightarrow A$) transition suggests that both the gain and the saturation energy density do not change significantly for injection pulse durations as short as 50 fs [23]. Scaling of the XeF($C \rightarrow A$) excimer system has been demonstrated successfully for nanosecond systems [18], and therefore the design of electron-beam pumped, large aperture systems, as demonstrated for the KrF excimer [4] should also be applicable to the XeF($C \rightarrow A$) excimer amplifier, increasing the performance of this system even further.

Acknowledgment

The authors would like to thank J. Hooten of Rice University for technical assistance.

References

[1] S. Szatmári, F.P. Schäfer, E. Müller-Horsche, and W. Mückenheim, "Hybrid dye-excimer laser system for the generation of 80 fs, 900 GW pulses at 248 nm," *Opt. Commun.*, vol. 63, pp. 305–309, 1987.
[2] J. R. M. Barr, N. J. Everall, C. J. Hooker, I. N. Ross, M. J. Shaw, and W. T. Toner, "High energy amplification of picosecond pulses at 248 nm," *Opt. Commun.*, vol. 66, pp. 127–132, 1988.
[3] A. J. Taylor, C. R. Tallman, J. P. Roberts, C. S. Lester, T. R. Gosnell, P. H. Y. Lee, and G. A. Kyrala, "High-intensity subpicosecond XeCl laser system," *Opt. Lett.*, vol. 15, pp. 39–41, 1990.
[4] S. Watanabe, A. Endoh, M. Watanabe, N. Sarukura, and K. Hata, "Multiterawatt excimer-laser system," *J. Opt. Soc. Amer. B*, vol. 6, pp. 1870–1876, 1989.
[5] J. H. Glownia, J. Misewich, and P. P. Sorokin, "169-fsec XeCl excimer amplifier system," *J. Opt. Soc. Amer. B*, vol. 4, pp. 1061–1065, 1987.
[6] W. Tighe, C. H. Nam, J. Goldhar, L. Meixler, J. Robinson, E. Valeo, and S. Suckewer, "Powerful subpicosecond KrF laser for X-ray laser development in the 1–5 nm region," *Proc. SPIE*, vol. 1229, Femtosecond to Nanosecond High-Intensity Lasers and Applications, pp. 29–39, 1990.
[7] T. S. Luk, A. McPherson, G. Gibson, K. Boyer, and C. K. Rhodes, "Ultrahigh-intensity KrF* laser system," *Opt. Lett.*, vol. 14, pp. 1113–1115, 1989.
[8] P. Maine, D. Strickland, P. Bado, M. Pessot, and G. Mourou, "Generation of ultrahigh peak power pulses by chirped pulse amplification," *IEEE J. Quantum Electron.*, vol. 24, pp. 398–403, 1988.
[9] C. Sauteret, D. Husson, G. Theill, S. Seznec, S. Gary, and A. Migus, "Generation of 20-TW pulses of picosecond duration using chirped-pulse amplification in a Nd:glass power chain," *Opt. Lett.*, vol. 16, pp. 238–240, 1991.
[10] M. Ferray, L. A. Lompré, O. Gobert, A. L'Huillier, G, Mainfray, C. Manus, A. Sanchez, and A. S. Gomes, "Multiterawatt picosecond Nd-glass laser system at 1053 nm," *Opt. Commun.*, vol. 75, pp. 278–281, 1990.
[11] F. G. Patterson, M. D. Perry, R. Gonzales, and E. M. Campbell, "Multiterawatt Nd:glass based on chirped-pulse amplification," *Proc. SPIE*, vol. 1229, Femtosecond to Nanosecond High-Intensity Lasers and Applications, pp. 2–18, 1990.
[12] J. D. Kmetec, J. J. Macklin, and J. F. Young, "0.5 terawatt, 125 femtosecond Ti:sapphire laser," *Opt. Lett*, vol. 16, pp. 1001–1003, 1991.
[13] P. B. Corkum and R. S. Taylor, "Picosecond amplification and kinetic studies of XeCl," *IEEE J. Quantum Electron.*, vol. 18, pp. 1962–1975, 1982.
[14] A. J. Taylor, T. R. Gosnell, and J. P. Roberts, "Ultrashort-pulse energy-extraction measurements in XeCl amplifiers," *Opt. Lett.*, vol. 15, pp. 118–120, 1990.
[15] S. Szatmári and F. P. Schäfer, "Comparative study of the gain dynamics of XeCl and KrF with subpicosecond resolution," *J. Opt. Soc. Amer. B*, vol. 4, pp. 1943–1948, 1987.
[16] T. E. Sharp, Th. Hofmann, C. B. Dane, W. L. Wilson, F. K. Tittel, P. J. Wisoff, and G. Szabó, "Ultrashort-laser-pulse amplification in a XeF($C \rightarrow A$) excimer amplifier," *Opt. Lett.*, vol. 15, pp. 1461–1463, 1990.
[17] F. K. Tittel, G. Marowsky, W. L. Wilson, Jr., and M. Smayling,

"Electron beam pumped broad-band diatomic and triatomic excimer lasers," *IEEE J. Quantum Electron.*, vol. 17, pp. 2268-2281, 1981.
[18] C. B. Dane, G. J. Hirst, S. Yamaguchi, Th. Hofmann, W. L. Wilson, Jr., R. Sauerbrey, F. K. Tittel, W. L. Nighan, and M. C. Fowler, "Scaling characteristics of the XeF($C \rightarrow A$) excimer laser," *IEEE J. Quantum Electron.*, vol. 26, pp. 1559-1568, 1990.
[19] N. Hamada, R. Sauerbrey, W. L. Wilson, Jr., F. K. Tittel, and W. L. Nighan, "Performance characteristics of an injection-controlled electron-beam pumped XeF($C \rightarrow A$) laser system," *IEEE J. Quantum Electron.*, vol. 24, pp. 1571-1578, 1988.
[20] T. E. Sharp, C. B. Dane, F. K. Tittel, P. J. Wisoff, and G. Szabó, "Tunable, high-power, subpicosecond blue-green dye laser system with a two-stage dye amplifier," *IEEE J. Quantum Electron.*, vol. 27, pp. 1221-1227, 1991.
[21] L. M. Frantz and J. S. Nodvik, "Theory of pulse propagation in a laser amplifier," *J. Appl. Phys.*, vol. 34, pp. 2346-2349, 1963.
[22] C. B. Dane, S. Yamaguchi, Th. Hofmann, R. Sauerbrey, W. L. Wilson, and F. K. Tittel, "Spectral characteristics of an injection-controlled XeF($C \rightarrow A$) excimer laser," *Appl. Phys. Lett.*, vol. 56, pp. 2604-2606, 1990.
[23] F. Kannari, "Theoretical study of subpicosecond pulse amplification in XeF($C \rightarrow A$)," submitted to *IEEE J. Quantum Electron.*
[24] W. Koechner, *Solid-State Laser Engineering.* New York: Springer-Verlag, 1976, p. 581.
[25] H. J. Lehmeier, W. Leupacher, and A. Penzkofer, "Nonresonant third order hyperpolarizability of rare gases and N_2 determined by third harmonic generation," *Opt. Commun.*, vol. 56, pp. 67-72, 1985.
[26] S. Yamaguchi, Th. Hofmann, C. B. Dane, R. Sauerbrey, W. L. Wilson, and F. K. Tittel, "Repetitively pulsed operation of an injection controlled high power XeF($C \rightarrow A$) excimer laser," *IEEE J. Quantum. Electron.*, vol. 27, pp. 259-262, 1991.
[27] G. Szabó, Z. Bor, and A. Müller, "Phase-sensitive single-pulse autocorrelator for ultrashort laser pulses," *Opt. Lett.*, vol. 13, pp. 746-748, 1988.
[28] D. Normand, M. Ferray, L. A. Lompré, O. Gobert, A. L'Huillier, and G. Mainfray, "Focused laser intensity measurement at 10^{18} W/cm^2 and 1053 nm," *Opt. Lett.*, vol. 15, pp. 1400-1402, 1990.
[29] R. W. Schoenlein, J.-Y. Bigot, M. T. Portella, and C. V. Shank, "Generation of blue-green 10 fs pulses using an excimer pumped dye amplifier," *Appl. Phys. Lett.*, vol. 58, pp. 801-803, 1991.

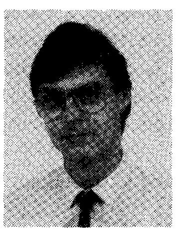

Thomas Hofmann was born in Hannover, Germany, on August 20, 1962. He received the M.S. degree in physics from the University of Hannover in 1988.

In 1989 he joined the Department of Electrical and Computer Engineering, Rice University, Houston, TX, where he is now a graduate student. His research interests include optical thin films and quantum electronics, specifically excimer laser physics and applications.

Tracy E. Sharp (S'89) was born in Tampa, FL, in 1966. She received the B.S. and M.S. degrees in electrical engineering from Rice University, Houston, TX, in 1988 and 1990, respectively.

She is presently working towards the Ph.D. degree in electrical engineering at Rice University.

Ms. Sharp is a member of Tau Beta Pi, Eta Kappa Nu, the IEEE Lasers and Electro-Optics Society, and the Optical Society of America.

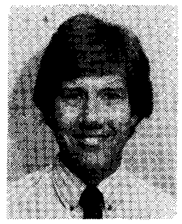

C. Brent Dane was born in Dalhart, TX, on August 8, 1961. He received the B.S. degree in chemistry and mathematics from Wayland Baptist University, Plainview, TX, in 1983 and the M.A. and Ph.D. degrees in physical chemistry from Rice University, Houston, TX, in 1986 and 1987, respectively.

From January 1988 to May 1990, he was a research associate with the Department of Electrical and Computer Engineering, Rice University. He is presently a staff physicist in the Laser Programs Division at Lawrence Livermore National Laboratory, Livermore, CA. His primary research activities have been in the development of tunable laser systems in the visible and infrared and their applications in spectroscopy and the study of chemical kinetics.

Dr. Dane is a member of Optical Society of America and Sigma Xi.

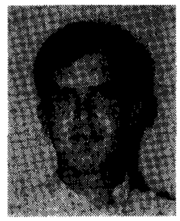

Peter J. Wisoff (M'86) was born in Norfolk, VA, on August 16, 1958. He received the B.S. degree in physics with highest distinction from the University of Virginia, Charlottesville, in 1980 and the M.S. and Ph.D. degrees in applied physics from Stanford University, Stanford, CA, in 1982 and 1986, respectively, as an NSF Graduate Fellow.

He has been with the Department of Electrical and Computer Engineering, Rice University, Houston, TX, since 1986 as an Assistant Professor. His research has focused on the development of short wavelength lasers, high intensity ultrafast lasers, and new excimer amplifier systems. In 1990, he was selected for the U.S. Astronaut Program at Johnson Space Center, Houston, TX.

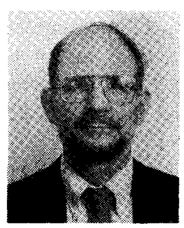

William L. Wilson, Jr. (S'68-M'71-SM'87) was born on February 6, 1943. He received the B.S. degree in 1965, the M.E.E. degree in 1966, and the Ph.D. degree in 1972, all in electrical engineering from Cornell University, Ithaca, NY.

From 1971 to 1972, he was an Instructor-Research Associate with the Electrical Engineering School at Cornell University. From 1972 to the present, he has been associated with the Department of Electrical and Computer Engineering, Rice University, Houston, TX, where he now holds the position of Professor. His research interests include tunable excimer lasers and solid-state devices.

Dr. Wilson is a member of Tau Beta Pi, Eta Kappa Nu, Sigma Xi, the IEEE Magnetics Society, the IEEE Microwave Theory and Techniques Society, the IEEE Electron Devices Society, and the American Physical Society.

Frank K. Tittel (SM'72-F'86), for a photograph and biography, see p. 394 of the February 1992 issue of this JOURNAL.

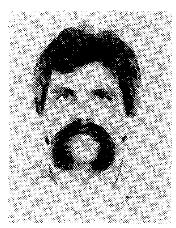

Gabor Szabó was born in Hungary in 1954. He received the M.S. and Ph.D. degrees in physics from JATE University, Szeged, Hungary, in 1978 and 1981, respectively.

From 1984 to the present, he has been at JATE University where he is an Associate Professor in the Department of Optics and Quantum Electronics. In addition he has been a Visiting Scientist at both the Max-Planck Institute, Göttingen, Germany, and Rice University, Houston, TX.

Dr. Szabó is a member of the Hungarian Physical Society.